

# **Comparison of Orbital Parameters for GEO Debris Predicted by LEGEND and Observed by MODEST: Can Sources of Orbital Debris be Identified?**

**E. S. Barker, M. J. Matney**

*National Aeronautics and Space Administration, Johnson Space Center, Mail Code KX,  
Houston, TX 77058, USA, 281-483-2591, FAX 281-483-5276, edwin.s.barker@nasa.gov*

**J.-C. Liou, K. J. Abercromby, H. M. Rodriguez, M. F. Horstman**

*ESCG, 2224 Bay Area Blvd, Houston, TX, 77058, USA*

**P. Seitzer**

*University of Michigan, Dept. of Astronomy, 818 Dennison Bldg. Ann Arbor, MI 48109-1042, USA*

## **ABSTRACT**

Since 2002, the National Aeronautics and Space Administration (NASA) has carried out an optical survey of the debris environment in the geosynchronous Earth-orbit (GEO) region with the Michigan Orbital Debris Survey Telescope (MODEST) in Chile. Under gravitational perturbations the distributions of uncontrolled objects, both Correlated (CTs) and Uncorrelated (UCTs) targets, in GEO orbits will evolve in predictable patterns, particularly evident in their inclination and right ascension of the ascending node (RAAN) distributions. There are several clusters ([1] have used a “cloud” nomenclature) in observed distributions that show evolution from year to year in their inclination and ascending node elements. Identification of the source(s) for these “clusters of UCTs” would be advantageous to the overall definition of the GEO orbital debris environment. This paper will present arguments for the identity of the source of the “clustering of UCTs” roughly centered on an inclination of  $12^\circ$  and a RAAN of  $345^\circ$ . The breakup of the Titan 3C-4 transtage on February 21, 1992 has been modeled using NASA’s LEGEND (LEO-to-GEO Environment Debris) code to generate a GEO debris cloud. Breakup fragments are created based on the NASA Standard Breakup Model (including fragment size, area-to-mass (A/M), and delta-V distributions). Once fragments are created, they are propagated forward in time with a subroutine GEOPROP (GEO Propagator). Perturbations included in GEOPROP are those due to solar/lunar gravity, radiation pressure, and major geopotential terms.

The question to be addressed: are the UCTs detected by MODEST in this inclination/RAAN region related to the Titan 3C-4 breakup? Discussion will include the observational biases in attempting to detect a specific, uncontrolled target during given observing session. These restrictions include: (1) the length of the observing session, which is 8 hours or less at any given date or declination; (2) the assumption of ACO elements for detected object when the breakup model predicts debris with non-zero eccentricities; (3) the size and illumination or brightness of the debris predicted by the model and the telescope/sky limiting magnitude. Possibly, one of the major restrictions is the primary focus of the MODEST program, which is to uniformly survey the GEO belt region and then move to declinations above and below the belt region as observing time permits.

## **1. INTRODUCTION**

### **1.1 Titan Breakup Event**

The breakup of the Titan 3C-4 transtage occurred on February 21, 1992 at an altitude of ~35,600 km, inclination (INC) of 11.9 degrees and a right ascension (RA) of 21.8 hours. The operator of the GEODSS sensor on Maui, Hawaii witnessed approximately 20 pieces in the breakup, but none were tracked at the time. Subsequent to the breakup the U. S. Space Surveillance Network (SSN) identified two pieces of the debris and assigned them to the catalogue as SSN 25000 and SSN 25001.

### **1.2 MODEST Survey**

Since 2001 the National Aeronautics and Space Administration (NASA) has carried out an optical survey of the debris environment in the geosynchronous (GEO) region with the Michigan Orbital Debris Survey Telescope (MODEST) in Chile. MODEST is a 0.6/0.9-m Schmidt telescope located at the Cerro Tololo Inter-American Observatory (CTIO) in Chile. A brief description of the system follows: for more details see [2,3]. The telescope is equipped with a thinned 2048 x 2048 pixel charge couple device (CCD) with a field of view (fov) of  $1.3^\circ$  square and

2.318 arc-second pixels. In a 5 second exposure through a broad R filter, a limiting magnitude of  $R = 18^{\text{th}}$  is reached with a signal to noise (S/N) of 10.

The survey coverage has been similar for 4 of the 5 years allowing one to follow the orbital evolution of Correlated Targets (CTs), both controlled and un-controlled objects, and Un-Correlated Targets (UCTs). However, when MODEST is in survey mode (field-of-view  $\sim 1.3^\circ$ ) it provides only short orbital arcs on the order of  $\sim 5$  minutes, which then can only be fit under the assumption of a circular orbit approximation (ACO) to determine the orbital parameters. These ACO elements are useful only in a statistical sense as dedicated observing runs would be required to obtain sufficient orbital coverage to determine a set of accurate orbital elements and then to follow their evolution.

The primary purpose of the MODEST system has been to operate in survey mode to uniformly sample the GEO belt and regions above and below on at least a semi-annual basis. In survey mode, the telescope tracks at the sidereal rate a fixed right ascension (RA) and declination (DEC) point close to the anti-solar point just outside of Earth shadow. The primary DEC chosen for each run is the declination of the GEO belt as seen from Cerro Tololo for that date. On additional nights the telescope is pointed at DEC positions above and below the GEO belt. The declinations are chosen with overlapping field of views (FOV) and usually are concentrated on regions known to have significant CT populations, hence potential debris sources. During the exposure the charge on the CCD is shifted backwards such that GEO objects appear as point sources or short streaks, and stars appear as fixed length streaks. During the 5.3 minutes it takes a station-keeping GEO object to drift across the FOV, 8 independent detections can be made. A minimum of 4 detections are required in this 5.3 minute window for a real object. All correlated objects are visually examined to guard against false detections.

### **1.3 Calculation of Orbital Parameters Assuming a Circular Orbit**

Fitting a set of angles-only observations has been a long-standing problem in astrodynamics since the early days of astronomy. Historically, orbits are defined by six-dimensional Kepler elements (there are several ways to represent these elements – all equivalent – but a typical set consists of the semi-major axis, eccentricity, inclination, ascending node, argument of perigee, and true anomaly, all at a given epoch). However, “moving around” in this six dimensional space to optimize a data fit presents a number of difficulties. Kepler elements have singularities in their derivatives, and even specialized “non-singular” elements have potential problems. There is a way of representing a state vector of an orbit that is non-singular, however, and that is by using Cartesian coordinates. There is a one-to-one correspondence between a six-dimensional Cartesian state vector (3 dimensions of position, 3 of velocity) and a set of Kepler elements. The 6-D Cartesian state vectors have continuous derivatives, unlike Keplerian elements, so it is easier to optimize the solution in “Cartesian space” and transform back into “Keplerian Space” after the fit is completed.

Our orbit fit program uses an all-purpose multidimensional optimization routine known as a simplex method taken from Numerical Recipes [4]. While not always the most efficient method, it is robust enough to use with any data configuration. For a set of short-arc observations, an epoch time is chosen (such as the epoch of the first observation). Different six-dimensional Cartesian vectors are tested by transforming each into Kepler orbits, propagating them to each observation time in the set of observations, and computing the differences between the predicted and observed look angle vectors. One obvious way to measure this difference is to take the arc cosine of the vector dot product of the two normalized look vectors. However, if the angle between the vectors is small, the dot-product is very close to 1.0, and can lead to round off problems. Instead, we use the vector difference between the two normal vectors. This gives an excellent approximation of the angle between the two vectors if they are sufficiently close and can be transformed into a positional error on the sky in arc seconds. The optimization routine “experiments” with various Cartesian coordinate configurations until the sum of the squares of the positional errors (DVEC) is minimized. DVEC is used as a measure of the accuracy of the fit in arcseconds.

Because the observation arcs are so short, there are in general a variety of different orbits (of varying eccentricity) that give relatively good fits to the data, making it difficult to determine a single optimal orbit with no constraints on the solution. Therefore, the current configuration of the software penalizes solutions by how far their eccentricities differ from zero. This penalty is added to the positional error described above, resulting in an optimized solution equivalent to the best-fit circular orbit to the data set. We define this best-fit circular orbit as the assumed circular orbit (ACO) solution because the software has severely penalized any solution where eccentricity is greater than 0.

Similarly, we define the Eccentric Orbit as one where the software penalties have been removed and the eccentricity has been allowed to vary.

## 2. LEGEND MODELING

### 2.1 Description of LEGEND

NASA's orbital debris evolutionary model LEGEND (LEO-to-GEO Environment Debris) is capable of simulating the historical and future debris populations in the near-Earth environment [5,6]. The historical part of LEGEND adopts a deterministic approach to mimic historical launches and known breakup events. Instead of modeling the whole environment, LEGEND can also be simplified to simulate an individual event, and has been chosen as the tool for providing predicted Titan fragments for this study. Once the breakup event is specified in LEGEND, fragments down to 1 mm in size are created with the NASA Standard Breakup Model, which describes the fragment size, area-to-mass ratio ( $A/M$ ), and velocity distributions [7]. All objects are propagated forward in time after breakup. Perturbations included in the GEO propagator, GEOPROP, include solar and lunar gravitational perturbations, solar radiation pressure, and Earth gravity-field zonal ( $J_2, J_3, J_4$ ) and tesseral ( $J_{2,2}, J_{3,1}, J_{3,3}, J_{4,2}, J_{4,4}$ ) perturbations. The simulated orbital elements and other physical properties of the fragments are stored in output files for additional post-processing analysis. Figs. 1 and 2 demonstrate the clusters of debris created with sizes greater than 10cm for the beginning of different years. The modeled Titan fragments described in this paper were generated from a special LEGEND simulation. A total of 10 Monte Carlo runs, where different random number sequences were used to select fragments in size, area-to-mass ratio, and delta velocity, were analyzed. Because the limiting magnitude or detectable size for MODEST is 60cm, 973 Titan fragments 60cm and larger were selected, and then propagated from the breakup date to 2002 day 40 for comparison with the MODEST UCT data.

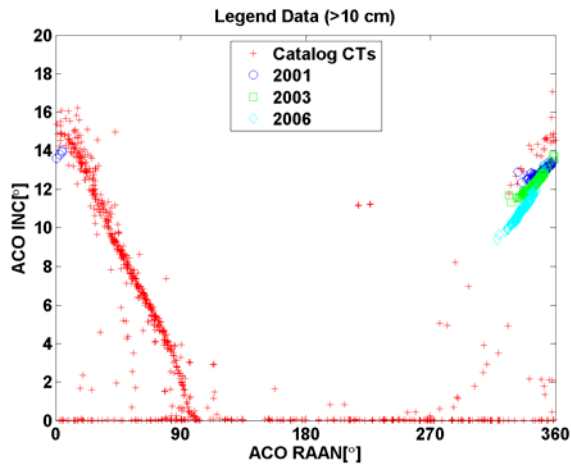


Fig. 1. Inc vs. RAAN plot of LEGEND simulated debris patterns for 2001, 2003, 2006 along with the Catalog elements for the observed CTs.

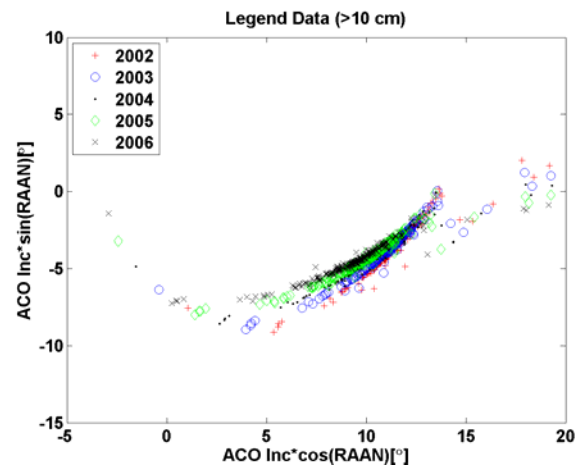
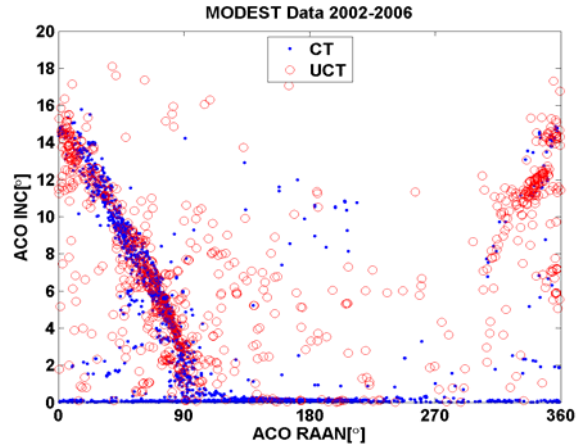


Fig. 2. Polar plot of potential debris patterns for 2002 through 2006 predicted by the LEGEND modeling.

## 3. MODEST DATASET

### 3.1 MODEST Observational Data Set

Using the actual Two Line Element (TLE) sets for the CTs and the ACO orbital elements for the UCTs, we plot the population distributions in different formats in Figs. 3 and 4. The GEO belt region is shown as the concentration of blue points on the horizontal axis with INC values less than  $0.1^\circ$ . The major feature seen in Fig. 3, starting at  $14^\circ$  INC and  $0^\circ$  RAAN and traveling through INCs to  $90^\circ$  RAAN, is caused by the precession of the orbital planes due to the Earth's oblateness plus the solar and lunar perturbations on the orbital planes. As uncontrolled CTs and debris are gravitationally perturbed their INCs increase and they move away from the GEO belt to a maximum inclination of about  $15^\circ$  over  $\sim 50$  years. This evolution is along predictable patterns, particularly evident in their inclination and right ascension of the ascending node (RAAN) distributions. Another way to display the INC and RAAN distributions is with a polar ( $X = \text{INC} \cdot \cos(\text{RAAN})$ ,  $Y = \text{INC} \cdot \sin(\text{RAAN})$ ) or the angular momentum plot as shown in Fig. 4 which is limited to just the UCTs or primarily debris targets.



**Fig. 3. MODEST CTs and UCTs for 2001-2006.**

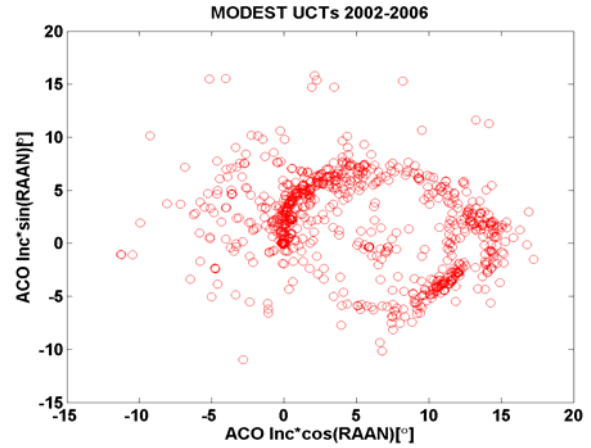


**Fig. 4. Polar plot of data presented in Fig. 3 but limited to just UCTs.**

There are several clusters (Schildknecht [1] has used a “cloud” nomenclature) in observed distributions that can be noted in the clustering of their inclination and ascending node elements as shown in Figs. 3 and 4. Identification of the source(s) for these “clusters of UCTs” would be advantageous to the overall definition of the GEO orbital debris environment. The remainder of this paper will present arguments for the identity of the source of the “clustering of UCTs” roughly centered on an  $INC=12^\circ$  and a  $RAAN=340^\circ$  as seen in Fig. 3 or in Fig. 4 near x and y values of  $11.6^\circ$  and  $-3.1^\circ$ , respectively. The parent body of the Titan breakup (SSN 3432) has values of  $INC=12.5^\circ$  and  $RAAN=346.56^\circ$  for a 2002 epoch. The LEGEND models (Figs. 1-2) predict debris in these regions of  $INC$  and  $RAAN$  distributions. The limited data MODEST UCT dataset is shown in Fig. 6 where the sample box is somewhat larger than the actual clustering of UCTs to make sure we are sampling all the possible UCT and LEGEND debris correlations. The  $INC$  and  $RAAN$  plot has the horizontal axis redefined to better illustrate the clustering around  $0^\circ$  or  $360^\circ$ .

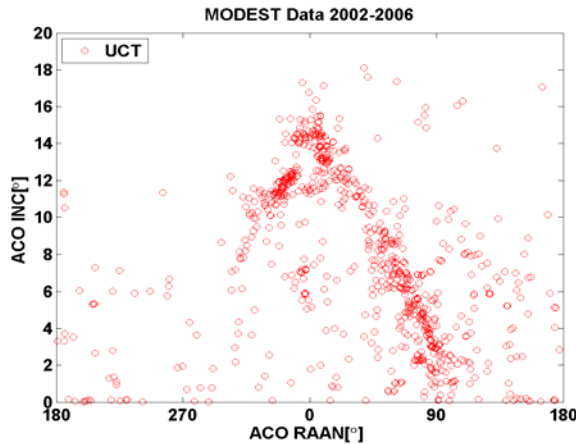


**Fig. 5. Inc vs. RAAN plot for all MODEST UCTs, same plot as Fig. 3 except for shifted horizontal axis.**

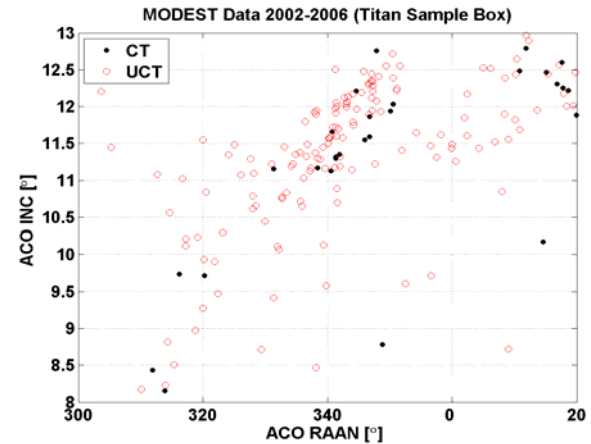


**Fig. 6. Inc vs. RAAN plot for all MODEST data, same plot as Fig. 6 but limited to the cluster around  $RAAN=340^\circ$ ,  $INC=12^\circ$ .**

Two pieces of the Titan debris have been designated as SSN 25000 and SSN 25001. However, MODEST has not observed either 25000, 25001 or the parent body SSN 3432 due to observational constraints driven by survey criteria listed in section 2.1. Simply stated, MODEST did not observe the exact GEO region in RA and DEC space where 25000 and 25001 were predicted to be during any of the survey observing runs. The primary focus of the MODEST program was to uniformly survey the GEO belt region and then move to declinations above and below the belt region as observing time permitted. Fig. 7 shows a typical case where MODEST was pointed at a given RA and DEC and the track (same epoch date) for 25000 is shown during the period when MODEST was taking data. Fig. 8

demonstrates another scenario where the track of 25000 passed at a significantly higher DEC than MODEST was observing. The tracks of 25000 shown in Figs. 7 and 8 are for periods where the debris was illuminated. The rest of the paper will be devoted to determining whether there were other times when Titan debris was detected.

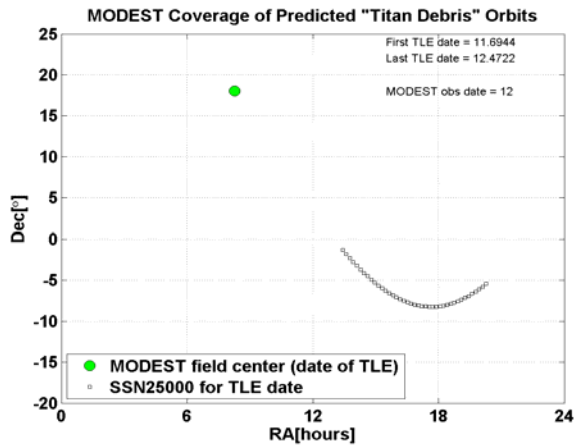


Fig. 7. Predicted positions for 25000 and position of MODEST FOV (symbol~1.3°) on DOY 012 2002.

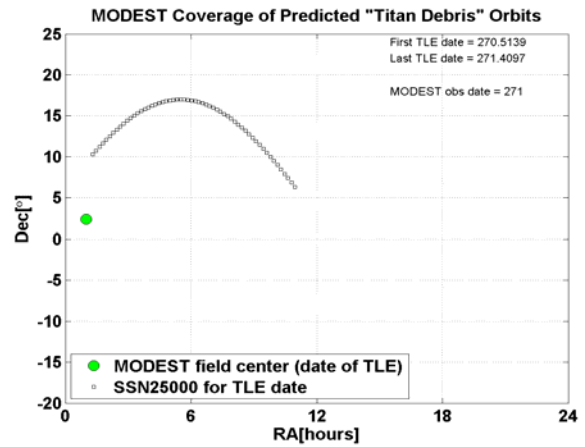


Fig. 8. Predicted positions for 25000 and position of MODEST FOV(symbol~1.3°) on DOY 271 2002.

Although the MODEST dataset includes 4 years of data, our initial investigation was limited to a single observational run in 2002 (DOY 40 through 52). The choice of this 12 day run was based on; (1) the length of the run, (2) several UCTs detected on many nights, (3) the center of the MODEST FOV varied and (4) the DEC was close to the track of the Titan debris as predicted by the LEGEND TLEs. Other observing runs will be analyzed in the future based on lessons learned and available time. The dates of the observing run and number of detected UCTs within the Titan sample box (Fig. 6) are listed in Table 1.

Table 1. MODEST Observations Used in this Analysis

DOY in 2002	Declination of MODEST FOV (°)	Observing Time (hours)	Total UCTs Detected	UCTs in Inc/RAAN sample box	UCTs along ACO tracks
40	07.2	7.22	3	0	0
41	08.4	7.15	5	2	1
42	08.4	7.12	3	1	0
44	09.6	7.19	8	2	1
45	10.8	6.86	3	2	2
46	12.0	6.93	4	3	3
47	08.4	6.17	3	0	0
48	09.6	5.98	8	0	0
49	10.8	5.98	8	3	3
50	12.0	5.39	11	7	5
51	13.2	5.52	11	5	4
52	14.4	4.88	4	4	2

#### 4. COMPARISON OF MODEST UCT ACO ORBITS WITH LEGEND TLE ORBITS

##### 4.1 Prediction of ACO Elements from LEGEND TLEs

In an attempt to answer the question on how to compare the UCTs ACO elements and the Legend Titan TLEs, software was developed to produce pseudo MODEST observations from positions derived from the LEGEND TLEs. LEGEND generated debris TLEs were produced for the observing run epoch and consisted of LEGEND modeled, Titan debris varying in size 0.6m to 1.5m via procedures outlined in section 2.1. Since the exact mean anomaly (MA) of the LEGEND produced TLE was unknown, a new TLE was produced at 4 degree increments in MA around the debris orbit. Each one of these TLEs was used to produce pseudo observational positions (RA and DEC) at the MODEST sampling rate (37.9 sec) during the MODEST observing session each night. At least 4 of these

pseudo positions were required to occur within the MODEST FOV to record a detection. Most detections contained at least 8 pseudo positions.

These detections were then processed to produce an ACO set of elements in a process parallel to that defined in section 1.3 for real CT and UCT observations. The final software product was a series of ACO elements for each LEGEND generated debris TLE. The number of ACO positions depended on the length of the orbital arc viewed by the MODEST during the night and the choice of a  $4^\circ$  increment in MA. The  $4^\circ$  increment was found to be the best compromise between number of detections and computing time required to process one night's set of TLEs which was still 8 to 10 hours for the  $4^\circ$  case. A sample of a single debris TLE and set of produced ACO elements is presented in Fig. 9 where  $\Omega$  is used instead RAAN. The upper pair of plots in Fig. 9 shows the INC vs. RAAN plot and the polar XY plot for a single night that has UCTs detected within the Titan sample INC/RAAN box in Fig. 6. The lower pair of plots are expanded scale plots of the upper plots needed to show the details of the ACO and TLE elements within the region of the Titan debris. Each red circle in Fig. 9 represents an ACO orbit determined for the MA value that produced a set of observable positions. Additionally in Fig. 9 the green diamonds are the observed UCT positions and the LEGEND generated debris TLEs are shown as black boxes.

In Figs. 10-18 the detected UCTs within the sample box are plotted from their ACO elements. Those UCTs falling along or within the "zone or general location" of the debris ACO elements are considered to be possible candidates for Titan debris. Note in Table 1 that 20 of the 29 UCTs within the Titan sample box are within the ACO zone defined by the Titan debris TLEs. Table 2 lists the 20 candidate UCTs with their ACO orbital elements. All of these UCTs can not be definitively identified as Titan debris, just because a UCT falls within the zone of Titan/ACO orbits, although it is very encouraging.

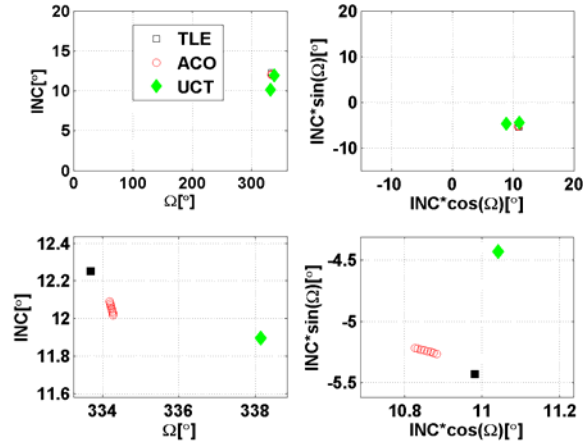


Fig. 9. Sample of a single debris TLE and the produced ACO elements on 2002 DOY 41.

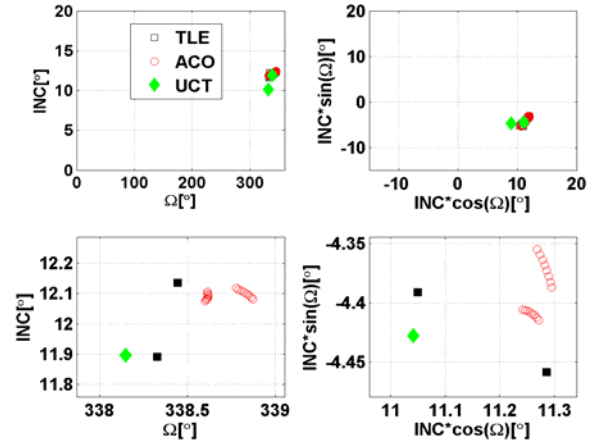


Fig. 10. All debris TLEs and their associated ACO elements on DOY 41.

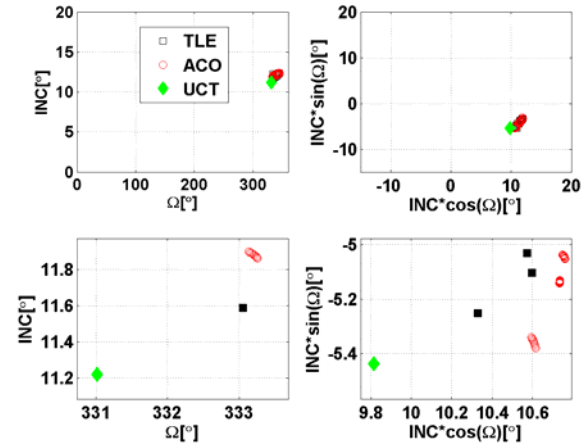


Fig. 11. All debris TLEs and their associated ACO elements for DOY 42.

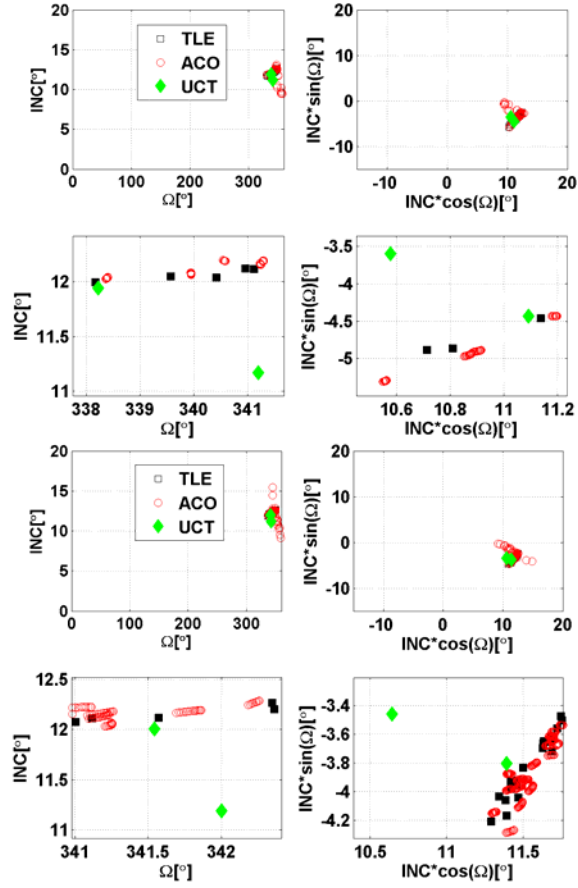


Fig. 13. All debris TLEs and their associated ACO elements for DOY 45.

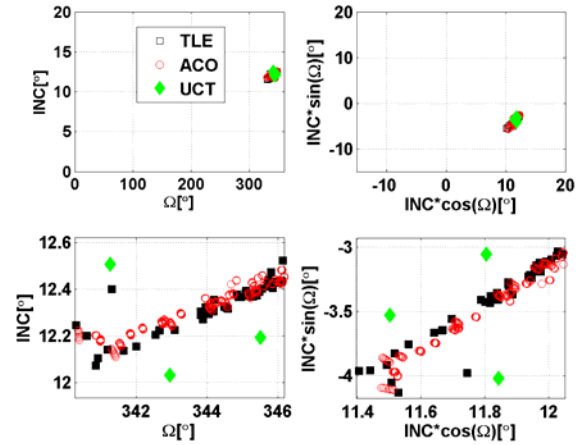


Fig. 15. All debris TLEs and their associated ACO elements for DOY 49.

Fig. 12. All debris TLEs and their associated ACO elements for DOY 44.

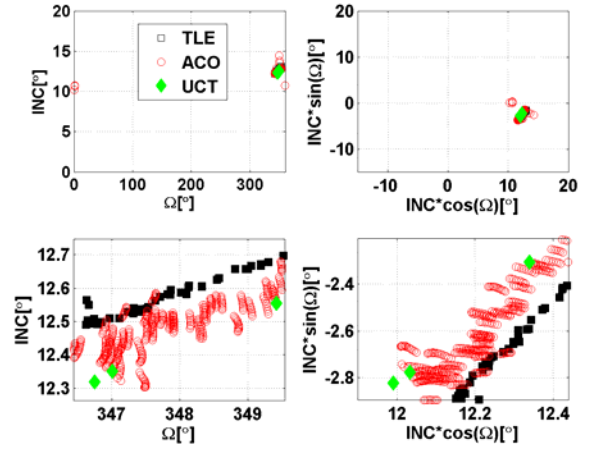


Fig. 14. All debris TLEs and their associated ACO elements for DOY 46.

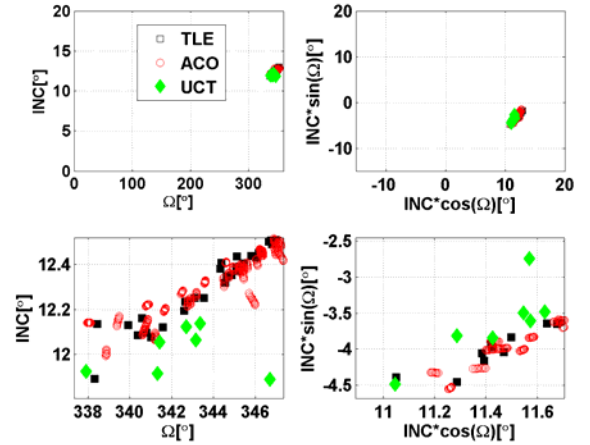


Fig. 16. All debris TLEs and their associated ACO elements for DOY 50.



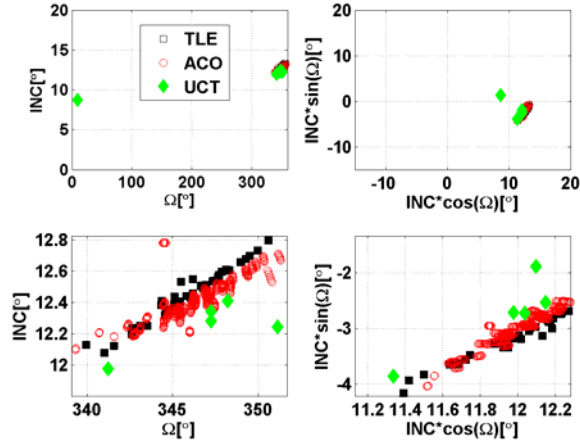


Fig. 17. All debris TLEs and their associated ACO elements for DOY 51.

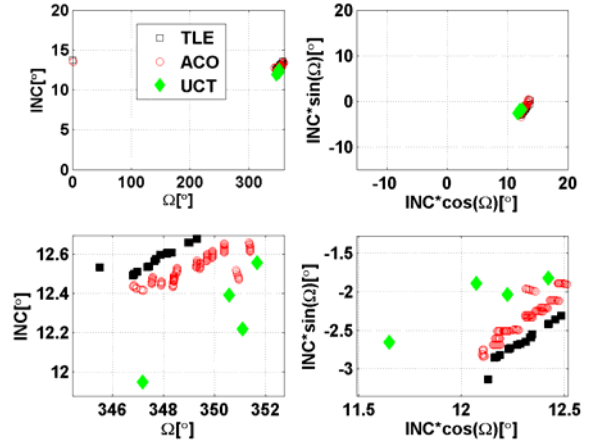


Fig. 18. All debris TLEs and their associated ACO elements for DOY 52.

Table 2. Candidate UCTs within the Titan Debris ACO Zones

Designation	Date	Obj	UT	ACO MM	ACO INC	ACO RAAN	ABSMAG	polar x	polar y
	yyyydoy	#	hrs	(°)	(°)	(°)	(R)	(°)	(°)
A	2002041	16	6.31267	1.0626	11.9	338.1	12.2	11.04	-4.43
B	2002044	10	4.74251	1.0640	11.9	338.2	12.1	11.09	-4.43
C	2002045	8	3.27702	0.9998	12.0	341.5	15.4	11.39	-3.80
D	2002046	7	3.97548	0.9985	12.3	346.8	16.6	11.99	-2.82
E	2002046	8	4.27032	0.9791	12.6	349.4	16.6	12.34	-2.31
F	2002046	9	4.39667	1.0305	12.4	347.0	14.8	12.03	-2.78
G	2002049	10	5.58199	1.0488	12.0	342.9	17.1	11.50	-3.53
H	2002049	12	6.44537	1.0137	12.2	345.5	16.6	11.80	-3.05
I	2002049	13	6.48748	0.9829	12.5	341.3	15.7	11.84	-4.02
J	2002050	1	1.281	1.0661	11.9	337.9	12.2	11.05	-4.49
K	2002050	3	2.20754	0.9945	12.1	341.4	15.4	11.43	-3.84
L	2002050	6	3.77638	1.0310	12.1	342.7	16.9	11.57	-3.60
M	2002050	9	4.08175	1.0212	12.1	343.4	16.5	11.63	-3.48
N	2002050	10	4.3029	1.0516	12.1	343.2	16.7	11.55	-3.49
O	2002051	2	1.50181	1.0688	12.0	341.2	17	11.34	-3.85
P	2002051	4	1.96508	1.0102	12.3	347.2	16.1	11.98	-2.71
Q	2002051	12	4.71314	1.0312	12.3	347.2	14.7	12.04	-2.72
R	2002051	15	5.55542	1.0241	12.4	348.2	16	12.15	-2.53
S	2002052	1	1.46475	1.0128	12.4	350.6	15.8	12.22	-2.03
T	2002052	2	1.77007	1.0115	12.6	351.7	16.2	12.42	-1.82

## 5. DISCUSSION OF CORRELATIONS



### 5.1 Correlation Between Candidate UCTs

As seen in Table 2, several UCTs have similar ACO orbital elements. In an attempt to link these UCTs between nights, orbit fits were carried out using the methods described in section 1.3 except the eccentricity was not forced to zero. Some combination resulted in good orbital fits (small values of DVEC in arcseconds, see section 1.3) and these orbits have similar orbital to Titan TLEs debris. Two night combinations for (AB, AJ, BJ, and CK, noted by color highlights in Table 2) gave DVEC values smaller than 20 arcseconds. One three night combination (ABJ) gave a DVEC value of 83 arcseconds.

### 5.2 Correlation Between All UCTs Observed During Run

To determine how much confidence to place in small values of DVEC, we fitted pairs of CT observations taken during the same observing run. Eccentric orbits were fit for 10 CTs with known TLEs. For those orbits with eccentricities less than 0.01, DVEC values were less than 20 arcseconds. Similarly, orbits with eccentricities between 0.01 and 0.2 had DVEC values less than 100 arcseconds. Using criteria that limited the possible UCT combinations to time spans of 4 nights or less, 89 combinations were fit having DVEC values ranging from 7 to 1415 arcseconds. Twenty five eccentric orbits determined for those combinations had DVEC values less than 100 arcseconds. Table 3 presents the possible UCT combination candidate orbits (5) that predict positions within the Titan debris sample box as defined in Fig. 6. The other 20 eccentric objects had predicted orbital position outside of the Titan debris sample box. All of the combinations presented in Table 3 have low values of DVEC, well within the limits defined for good orbits by observations and eccentric orbit fitting of the CTs during this observing run.

**Table 3. Eccentric Orbit Fits for Pairs of Candidate UCTs within the Titan Debris Sample Box**

Combo	MM	Ecc	INC	RAAN	AP	MA	DVEC
	(d)		(°)	(°)	(°)	(°)	(arcsec)
AB	1.0192	0.1218	13.2	336.3	246.1	292.3	18
IO	1.1000	0.1840	11.2	343.5	40.8	91.1	22
IK	1.1833	0.1783	10.2	346.9	15.9	116.8	26
GL	1.0696	0.0241	11.2	345.4	6.9	140.5	27
GO	1.0801	0.1054	9.9	349.5	40.4	92.7	40

## 6. SUMMARY

LEGEND created TLEs, for the Titan breakup, that have been used to identify possible UCTs which could be Titan debris observed by MODEST in 2002 between DOY 40 and 52. Five UCTs have ACO orbits which are similar to the Titan debris ACO orbits and have positions along the zone of ACO orbits for modeled Titan debris. Additionally, fitting of night-to-night observations of UCTs with eccentric orbits resulted in 5 combinations of UCTs with low values of DVEC and orbital elements that were within the Titan debris sample box. While these fits are not definitive, they are quite encouraging that we have been able to link at least one and maybe 4 UCTs with Titan debris.

Future work will analyze 5 other MODEST datasets and carryout the definitive identification test by seeing if we can propagate any candidate UCT orbit back to the actual breakup date and position. To accomplish this identification we will need to dedicate a MODEST run to observing a GEO region predicted to contain debris fragments and actual debris objects (SSN 25000 and 25001).

## 7. REFERENCES

1. Schildknecht, T., et al., Optical Observations of Space Debris in High-Altitude Orbits, *Proceedings of the Fourth European Conference on Space Debris*, ESA SP-587, Darmstadt, Germany, 113 - 118, 2005.
2. Seitzer, P., et al., A Survey for Space Debris in Geosynchronous Orbit., *Proceedings of AMOS 2001 Technical Conference*, Maui, Hawaii, 2001.
3. Seitzer, P., et al., Results from the NASA/Michigan GEO Debris Survey, *Proceedings of AMOS 2004 Technical Conference Proceedings*, Maui, Hawaii, 2005.
4. *Numerical Recipes in Fortran 77 The Art of Scientific Computing*, 2<sup>nd</sup> Edition, Vol. 1, Cambridge University Press, p 403, 1992.

5. Liou, J.-C., et al., Hall, D.T., Krisko, P.H., Opiela, J.N. LEGEND – A three-dimensional LEO-to-GEO debris evolutionary model, ADV. SPACE RES., Vol. 34, No. 5, 981-986, 2004.
6. Liou, J.-C., Collision Activities in the future orbital debris environment. ADV. SPACE RES., ([doi:10.1016/j.asr.2005.06.021](https://doi.org/10.1016/j.asr.2005.06.021)), in press, 2006.
7. Johnson, N.L., et al., NASA's new breakup model of EVOLVE 4.0, ADV. SPACE RES., Vol. 28, No. 9, 1377-1384, 2001.